iScience

CellPress
OPEN ACCESS

Article

Monitoring Alzheimer's disease via ultraweak photon emission

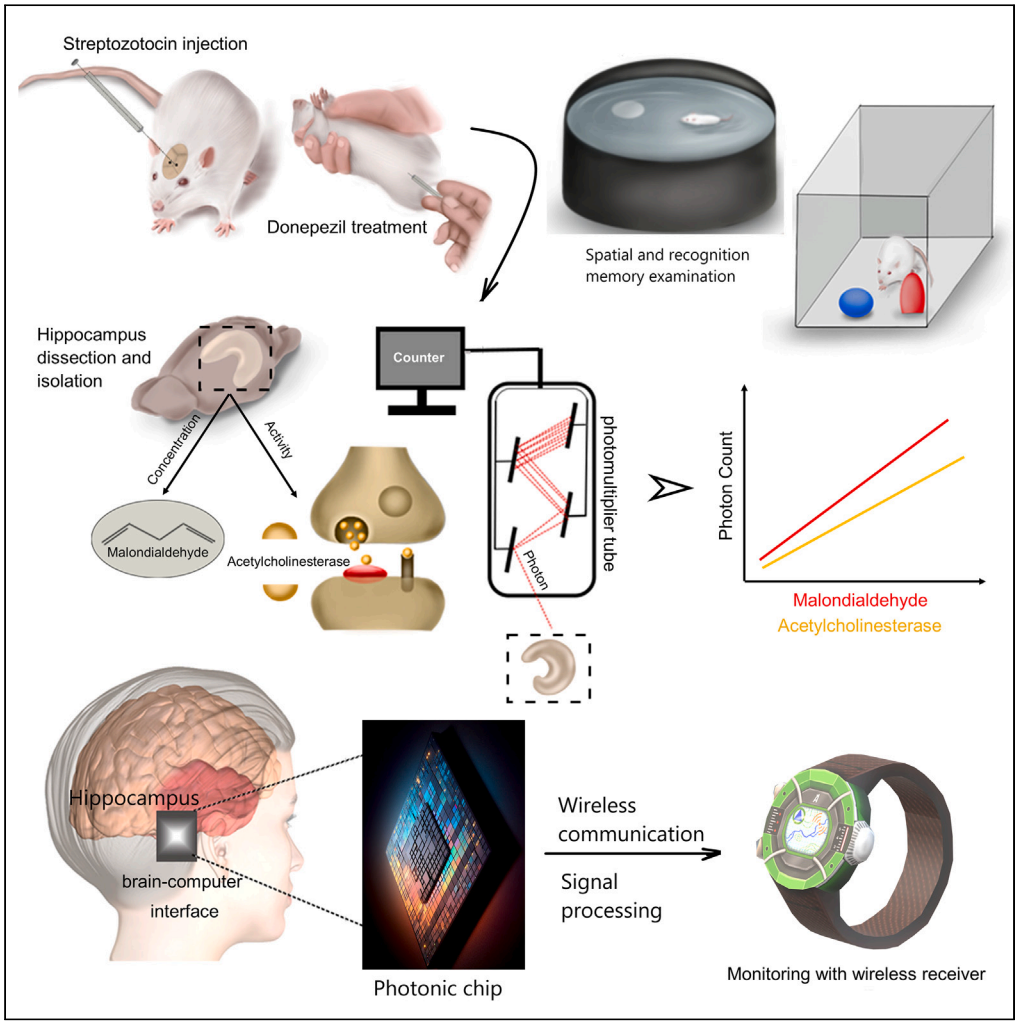

Niloofar Sefati, Tahereh Esmaeilpour, Vahid Salari, ..., István Bókkon, Serafim Rodrigues, Daniel Oblak

vahid.salari1@ucalgary.ca (V.S.)
srodrigues@bcamath.org (S.R.)
doblak@ucalgary.ca (D.O.)

Highlights

Elevated hippocampal UPE levels in STZ-injected rats: Insights into tissue redox dynamics

Donepezil reduces UPE and enhances neuroprotection in STZ-injected rats

Linking hippocampal UPE to oxidative stress and acetylcholinesterase activity

A potential revolutionary monitoring Alzheimer's disease via photonic chips

Sefati et al., iScience *27*, 108744
January 19, 2024
https://doi.org/10.1016/j.isci.2023.108744

iScience

CellPress
OPEN ACCESS

Article

Monitoring Alzheimer's disease via ultraweak photon emission

Niloofar Sefati,[1,12,13] Tahereh Esmaeilpour,[1,12] Vahid Salari,[2,3,4,*] Asadollah Zarifkar,[5] Farzaneh Dehghani,[1,6] Mahdi Khorsand Ghaffari,[5] Hadi Zadeh-Haghighi,[2,3,4,11] Noémi Császár,[7] István Bókkon,[7,8] Serafim Rodrigues,[9,10,*] and Daniel Oblak[2,3,4,*]

SUMMARY

In an innovative experiment, we detected ultraweak photon emission (UPE) from the hippocampus of male rat brains and found significant correlations between Alzheimer's disease (AD), memory decline, oxidative stress, and UPE intensity. These findings may open up novel methods for screening, detecting, diagnosing, and classifying neurodegenerative diseases, particularly AD. The study suggests that UPE from the brain's neural tissue can serve as a valuable indicator. It also proposes the development of a minimally invasive brain-computer interface (BCI) photonic chip for monitoring and diagnosing AD, offering high spatiotemporal resolution of brain activity. The study used a rodent model of sporadic AD, demonstrating that STZ-induced sAD resulted in increased hippocampal UPE, which was associated with oxidative stress. Treatment with donepezil reduced UPE and improved oxidative stress. These findings support the potential utility of UPE as a screening and diagnostic tool for AD and other neurodegenerative diseases.

INTRODUCTION

To the best of our knowledge, there is currently no brain implantable chip that is specifically designed to screen and diagnose Alzheimer's disease (AD). While implantable brain chips have been developed for various purposes such as monitoring brain activity or delivering therapeutic electrical stimulation, their use for screening or diagnosing AD is still an area of active research. Diagnosing AD typically involves a combination of cognitive and memory tests, brain imaging studies, and other assessments performed by a clinician. Based on the observation that the brain spontaneously emits photons, so-called ultraweak photon emissions (UPEs),[1,2] we suggest that a brain-computer interface with an integrated photonic chip (BCIPC)[3] may be an efficient real-time method for monitoring early symptoms of AD and related dementias (ADRDs). The envisaged technology would support clinicians by providing complementary data to efficiently screen and diagnose AD. Indeed, we have previously discussed a pattern recognition approach for an efficient interpretation of UPE via the output signals on a photonic interferometer chip.[3] Supporting this vision is the fact that various research studies have shown that there are significant UPEs from neurons across the electromagnetic spectrum.[1,4] Such UPEs reflect cellular (and brain) oxidative status, as they are particularly intense during heightened metabolic activity or stress.[5] Several studies point to direct correlations between UPE intensity and neural activity, oxidative reactions, EEG activity, cerebral blood flow, cerebral energy metabolism, and glutamate release.[6] Such correlations suggest that we may use UPEs as a correlative signal to monitor different internal states across the stages of ADRD pathology and to expand the clinical criteria, particularly in the preclinical and mild cognitive impairment (MCI) stages where memory loss and other problems are not always evident. Discrimination between the interferometric patterns of normal, and preclinical stages will be non-trivial but tractable via machine learning, based on observation of highly synchronized brain activities with strong UPE correlations for specific cognitive tasks.[3] With an analysis of signals over thousands of training trials, it will be possible to obtain an average pattern for feature extraction, enabling pattern recognition directly during preclinical and premarket approval testing.

[1]Department of Anatomical Sciences, School of Medicine, Shiraz University of Medical Sciences, Shiraz, Iran
[2]Department of Physics and Astronomy, University of Calgary, Calgary, AB, Canada
[3]Institute for Quantum Science and Technology, University of Calgary, Calgary, AB T2N 1N4, Canada
[4]Quantum Alberta, University of Calgary, Calgary, AB T2N 1N4, Canada
[5]Department of Physiology, School of Medicine, Shiraz University of Medical Sciences, Shiraz, Iran
[6]Histomorphometry and Stereology Research Center, Shiraz University of Medical Sciences, Shiraz, Iran
[7]Psychosomatic Outpatient Clinics, Budapest, Hungary
[8]Vision Research Institute, Neuroscience and Consciousness Research Department, Lowell, MA, USA
[9]MCEN Team, Basque Center for Applied Mathematics, Bilbao, Bizkaia, Spain
[10]IKERBASQUE, Basque Foundation for Science, Plaza Euskadi 5, 48009 Bilbao, Spain
[11]Hotchkiss Brain Institute, University of Calgary, Calgary AB T2N 1N4, Canada
[12]These authors contributed equally
[13]Lead contact
*Correspondence: vahid.salari1@ucalgary.ca (V.S.), srodrigues@bcamath.org (S.R.), doblak@ucalgary.ca (D.O.)
https://doi.org/10.1016/j.isci.2023.108744

The hippocampus is an important brain region that plays a crucial role in forming and retrieving memories.[7] In AD, one of the earliest symptoms is memory loss and difficulty in forming new memories, which is linked to hippocampus damage. Indeed, atrophy and shrinkage occur in the hippocampus of AD patients, which can be seen on brain scans such as MRI. However, it's important to note that memory loss and changes in the hippocampus can be caused by other factors as well, so it's not a definitive diagnostic tool for AD, hence a number of clinical evaluations are undertaken to accurately diagnose AD.

The detection of biophotons through a photonic chip implanted in the hippocampus is an area of ongoing research, and its potential for diagnosing AD is still unclear. Biophotons are extremely weak light emissions from biological systems and their relationship to neurodegenerative diseases such as AD is not yet fully understood, and there is currently no evidence to support its use as a reliable diagnostic tool for AD. This motivates the present study where we investigate biophotons from the hippocampus[8] and correlate it with other neuropathological signatures of AD, results of which enable us to propose a future development of BCIPC for screening and diagnosing AD.

Alzheimer's disease, ROS, and ultraweak photon emission

AD is the most common type of dementia and is a progressive neurodegenerative brain disorder causing a significant disruption of normal brain structure and function.[9] Sporadic Alzheimer's disease (sAD), which begins after the age of 65 without a family history, is the most common type of AD and has several causes and risk factors.[10] The risk factors and reasons associated with sAD include the accumulation of amyloid plaques, the formation of neurofibrillary tangles, decreased activity or the number of cholinergic neurons in the brain, neuroinflammation, insulin signaling impairments, mitochondrial disorders, and oxidative stress.[11,12] In the brain of an AD patient, the most consistent neurotransmitter-related change is the reduction of cholinergic innervation in the cortex and hippocampus caused by the loss of neurons in the basal forebrain.[13] Among the pharmacological agents, acetylcholinesterase (AChE) inhibitors, like donepezil, seem to be the most effective agent for improving cholinergic deficits and reducing the symptoms of AD.[14] As the most potent approved drug, donepezil affects various events of AD, such as inhibiting cholinesterase activities, anti-Aβ aggregation, anti-oxidative stress, etc.[15] In sAD, the initiating causes of the neurodegenerative cascade are unknown, but some studies suggest increased levels of oxidative stress and impaired energy metabolism as the initiating cause of the disease.[16] Oxidative stress is an imbalance between the antioxidant defense system and the production of reactive oxygen species (ROS). Mitochondria are susceptible to oxidative damage despite the presence of an antioxidant system, and damaged mitochondria produce more ROS than ATP.[17] Spontaneously, when ROS are produced during the metabolic processes, the ultraweak photons are emitted through the relaxation of electronically excited species formed during the oxidative metabolic processes[18]; therefore, the biophoton emission rate could be utilized in order to investigate tissue oxidative state.[19] The UPE produces a very weak luminescence and can be performed by living organisms,[18,20] comprising microorganisms, plants, and humans. It is mainly named biophoton emission.[21,22] The UPE intensity changes are related to different physiological and pathological conditions, such as different kinds of stress, mitochondrial respiratory chain, cell cycle, and cancerous growth. It has been shown that the measurement of delayed luminescence emitted from the tissues provides valid and predictive information about the functional status of biological systems.[23,24] Several studies repeatedly illustrated that the intensity of photon emission changes in an abnormal condition, and abnormal cells emit significantly more biophotons than healthy cells. It has also been shown that changes in biophotonic activity are indicative of changes in mitochondrial ATP energy production manifested in physiological and pathological conditions.[25,26] Having considered that ROS production is related to inflammatory diseases and impaired metabolic processes,[27] it is reasonable to expect that UPE can also be associated with inflammatory disease and/or metabolic processes.[28] Therefore, UPE might be used practically for the diagnosis of inflammation and inflammation-related diseases.[28] Reports have considered UPE as a potential diagnostic tool, and some studies have found evidence for diagnosing patients with type 2 diabetes[29] and breast cancer.[30]

Transgenic mouse models are associated with familial AD, which is observed in approximately 5% of AD patients, while the remaining 95% of AD cases are sporadic in nature. However, despite the promising results obtained in transgenic animal models, the majority of new drug candidates approved based on these models have failed to show efficacy in clinical studies. Many studies target mechanisms that aim to improve the obvious symptoms described in the pathogenesis of AD. Nevertheless, due to the lack of consideration for the underlying disturbances causing these symptoms, the error rate in drug development remains high.[31,32] Our study focused on non-transgenic mouse models associated with non-familial AD due to metabolic perturbation. It is essential to recognize that the current transgenic mouse models of AD do not fully replicate the entire disease course, which includes plaque and tangle formation, cognitive decline, synaptic loss, and progressive neurodegeneration. Even when expressing familial AD (FAD)-linked mutations, these mouse models fail to encompass all pathological pathways observed in humans. Ref. [33,34] provide a summary of brain pathology similarities between the icv-STZ rat model and human cases of sporadic AD. Furthermore, we encountered challenges when manipulating the hippocampus in mice, as compared to rats. The dissection of the mouse hippocampus requires swiftness, and larger tissue samples are preferred for better detection of UPE signals. Intracerebroventricular (ICV) injection of low doses of streptozotocin (STZ) leads to neuropathological, biochemical, and behavioral changes similar to non-hereditary sAD in the rat brain, so it is used as a laboratory model to investigate the process and treatment of sAD in rat brain.[35] STZ possibly desensitizes neuronal insulin receptors and reduces the activities of the glycolytic enzyme.[36] It causes oxidative stress and decreases cerebral energy metabolism resulting in cognitive dysfunction by inhibiting the synthesis of adenosine triphosphate (ATP) and acetyl CoA, which in turn leads to cholinergic deficiency supported by reduced choline acetyltransferase (ChAT) activity in the hippocampus[37,38] and increased AChE activity in rat whole brain.[39] To investigate the metabolic-centric aspect of AD, we employed the icv-STZ model in rats. It has been demonstrated that icv-STZ induces neuropathological, biochemical, and behavioral changes similar to non-hereditary Alzheimer's disease (sAD) in the rat brain. This model serves as a valuable laboratory tool to study the processes and potential treatments for sAD. Particularly, the icv-STZ model is associated with glucose utilization disorders and subsequent changes in energy metabolism. Importantly, these

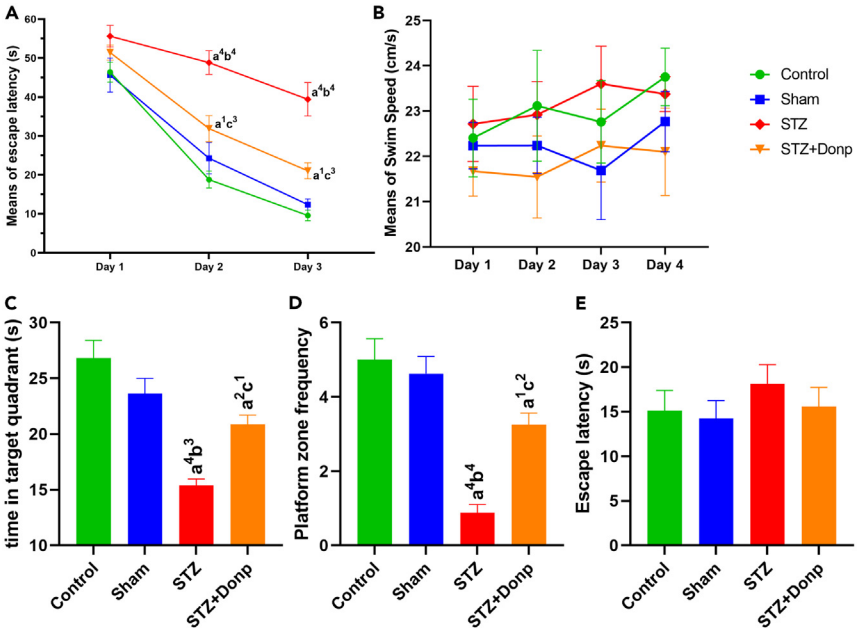

Figure 1. Morris water maze test

(A) Line chart of block mean of escape latency in trial days.

(B) Line chart of velocity in trial day.

(C) The target quadrant time spent in the probe trial.

(D) The platform zone crossing frequency in the probe trial.

(E) Escape latency in visible platform trial. Data were expressed as mean ± SEM (n = 8) and analyzed by two-way. Repeated measures ANOVA for acquisition trial and velocity, and one-way ANOVA for probe and visible trial followed by Tukey's multiple comparison test. (a), Compared to the control group; (b), Compared to the sham group; and (c), Compared to the STZ group; 1p < 0.05, 2p < 0.01, 3p < 0.001, 4p < 0.0001. STZ: Streptozotocin, Donp: Donepezil.

metabolic disruptions occur earlier than cognitive impairment and plaque formation in AD patients.[40–42] The rationale behind our focus on AD was the exclusive measurement of memory and hippocampus markers, as well as the utilization of UPE. Additionally, we put forward an innovative proposal for monitoring the brain's temporal lobe. However, due to the specificity of our results to the hippocampus, our discussion did not extend to other brain diseases. It is essential to note that morphological changes observed in Alzheimer's patients encompass enlarged brain ventricles and progressive medial temporal lobe atrophy, which becomes more pronounced as the disease advances. Brain MRI assessments of Alzheimer's patients have consistently indicated that hippocampal atrophy occurs earlier than in other brain regions.[43] The present study aims to evaluate the UPE intensity of the hippocampus in the normal, pathological, and therapeutic state and also investigate the relationships between the intensity of UPE, memory, oxidative stress, and AChE activity for AD diagnosis and treatment success.

RESULTS

Morris water maze

There was no significant difference in escape latency between groups on the first day of the acquisition trial. On the 2nd and 3rd days, there was a significant difference in escape latency between the control group and other groups (STZ $p < 0.0001$, STZ+Donp $p < 0.05$). STZ group had significantly higher scape latency in comparison with the sham group ($p < 0.0001$). Also, on this day, the escape latency of the STZ+Donp group significantly decreased in comparison with the STZ group ($p < 0.001$). Our results demonstrated that escape latency in the donepezil-treated group was significantly lower than in the STZ group ($p < 0.001$) (see Figure 1A). No significant differences were observed in swim speed between groups on all days of the trial (Figure 1B). In the probe trial, the STZ-injected groups significantly spent lower time in the target quadrant compared with the control group (STZ $p < 0.0001$, STZ+Donp $p < 0.01$). Still, only the STZ group was significant with the sham group ($p < 0.001$). Whereas the donepezil-treated group significantly spent higher time in the target quadrant in comparison with the STZ group ($p < 0.05$) (Figure 1C). In this trial, platform zone crossing in the STZ group significantly decreased compared with the control and sham groups ($p < 0.0001$). Moreover, the STZ+Donp group had a significant difference from the STZ group ($p < 0.01$) and the control group ($p < 0.05$) (Figure 1D). Escape latency in visible platform trials was not significantly different between the groups (Figure 1E).

Novel object recognition test

No differences in the spent time exploring the two identical objects during the familiarization phase were found among animals (Figure 2A). ICV-STZ injection impaired responding in the NOR test, as was indicated by failure to discriminate between familiar and novel objects during

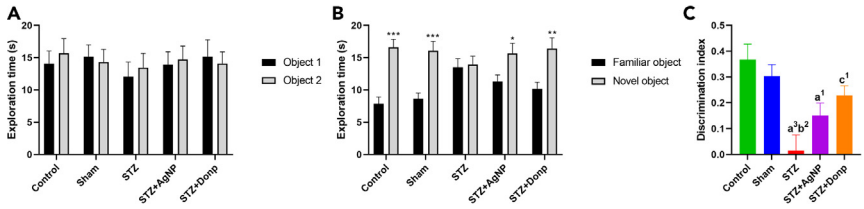

Figure 2. Novel object recognition test

(A) Exploration time during the familiarization phase.

(B) Exploration time during the testing phase.

(C) Discrimination index. Data were expressed as mean ± SEM (n = 8) and analyzed by paired t-test. *p < 0.05, **p < 0.01, ***p < 0.001 compared to the exploration time of familiar objects during the testing phase of respective groups. Data were analyzed by one-way ANOVA followed by Tukey's multiple comparison tests. (a), Compared to the control group; (b), Compared to the sham group; (c), Compared to the STZ group; 1p < 0.05, 2p < 0.01, 3p < 0.001. STZ: Streptozotocin, Donp: Donepezil.

the testing phase 1 h after the familiarization phase. In control and sham groups, a significant increase ($p < 0.001$) in exploration time toward a novel object was observed in comparison with a familiar object. Administration of donepezil improved memory in STZ-injected rats, as was shown by a significant increase ($p < 0.01$) in the exmeansation time of the novel object compared with the familiar object (Figure 2B). When results were expressed as discrimination index, the STZ group had a significantly lower discrimination index compared with control and sham groups ($p < 0.01$, and $p < 0.001$ respectively), two-way ANOVA analyzed data significantly higher discrimination index in comparison with the STZ group ($p < 0.05$) (Figure 2C).

Photon emitting evaluation of the hippocampus

The mean of the total photon emission of the hippocampus during the 300 s was shown in Figure 3. ICV-STZ injection significantly increased hippocampus photon emission of STZ-injected rats compared with control and sham groups ($p < 0.0001$). The STZ+Donp rats had significantly lower hippocampus photon emission in comparison with the STZ group rats ($p < 0.01$).

Hippocampus MDA concentration

MDA concentration (index of lipid peroxidation) in the STZ-injected groups was significantly higher than in control and sham groups ($p < 0.0001$). Also, lipid peroxidation decreased in the STZ+Donp group ($p < 0.001$) compared with the STZ group but was still significant with control and sham groups ($p < 0.001$, $p < 0.05$, respectively) (Figure 4).

AChE activity of the hippocampus

The hippocampal AChE activity significantly ($p < 0.0001$) increased in the STZ-group compared with control and sham groups. In the donepezil-treated group, AChE activity of the hippocampus significantly decreased in comparison with the STZ group ($p < 0.01$) but had significantly higher AChE activity than in the control group ($p < 0.01$) (Figure 5).

Correlation matrix of UPE with MDA & AChE activity of the hippocampus

UPE had more correlation strange with MDA as was proven by Pearson correlation analysis, UPE vs. MDA ($r = 0.8552$); UPE vs. AChE activity ($r = 0.7793$). The Coefficient of determination (r2) in this analysis showed that 73% of the UPE variance could be explained by MDA concentration, while 60% of UPE variance could be explained by AChE activity (Figure 6).

DISCUSSION

To the best of our knowledge, this is the first study that investigates UPE emission from the hippocampus as a potential clinical tool for the diagnosis of sporadic AD. The focus of our discussion on AD was primarily on memory and hippocampus markers, as well as the utilization of UPE measurements. Furthermore, we proposed an innovative approach for monitoring the temporal lobe of the brain. Alzheimer's patients exhibit morphological changes in their brains, including enlarged brain ventricles and progressive medial temporal lobe atrophy, which worsens as the disease advances. Notably, hippocampal atrophy is observed earlier than in other brain regions during brain MRI assessments of Alzheimer's patients.[43] Due to the specificity of our results to the hippocampus, we were unable to delve into other brain diseases, such as Parkinson's, which is associated with brain striatum and dopaminergic neurons, as we primarily measured hippocampus and cholinergic activity. Additionally, we evaluated memory impairment, the main symptom of AD, and found no evidence of mobility impairment, as demonstrated by the absence of significant differences in swim speed between rats during the MWM test. Our focus was solely on measuring UPE-related markers, specifically assessing the hydrolysis chemical reaction related to UPE, where AChE hydrolyzes Ach. Additionally, MDA serves as a marker for lipid peroxidation, providing insights into the oxidative metabolic state of the tissue. The generation of UPE occurs through redox reactions, involving the transfer of electrons between species and resulting in orbital changes. The reason for

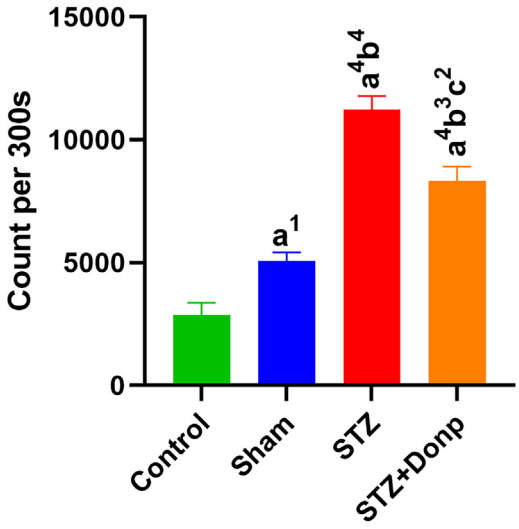

Figure 3. Representation of hippocampus total photon emission during the 300 s
The result was expressed as mean ± SEM (n = 8). Data were analyzed by one-way ANOVA followed by Tukey's multiple comparison test. (a), Compared to the control group; (b), Compared to the sham group; (c), Compared to the STZ group; 1p < 0.05, 2p < 0.01, 4p < 0.0001. STZ: Streptozotocin, Donp: Donepezil.

emphasizing AD in our study was to evaluate memory impairments and their correlation with hippocampus markers and UPE. Memory impairment stands as the principal and initial symptom of AD, and the hippocampus plays a crucial role in AD pathogenesis and memory deficits. SAD is recognized as a multifactorial condition with several risk factors, including vascular and metabolic impairments, nutritional deficiencies, depression, brain trauma, and genetic factors (such as apolipoprotein E).[44] Consequently, any disorder that could lead to brain damage, especially in the hippocampus, is considered a risk factor for AD. Biologically, all damage in AD originates from oxidative stress or metabolic changes. For instance, neuroinflammation prompts microglia and astrocytes to release significant amounts of superoxide via NADPH oxidase, resulting in cytotoxicity to nearby injured cells and ultimately leading to apoptosis. Amyloid plaque alone may not induce damage, but when surrounded by neuroinflammation, it leads to oxidative damage. Notably, brain metabolism imbalance and oxidative stress precede the formation of amyloid plaques and neurofibrillary tangles, indicating that oxidative stress may be a primary event in AD progression.[28,45] Moreover, an excessive increase in BACE1 activity and levels, related to amyloid-beta, has been observed in the brains of both mice and humans. Reports suggest that the BACE1 promoter includes stress-sensitive genome areas and proinflammatory cytokines, further linking AD pathology to oxidative stress and inflammation.[29,46] To test the viability of the proposed diagnostic tool we focused on ICV-STZ-induced sporadic AD models and compared with control, Sham and ICV-STZ rats treated with the most potent treatment of AD (donepezil).

In this research, specifically, we analyzed the associations between memory, oxidative stress, AChE activity, and UPE intensity of the hippocampus. Following ICV administration of STZ, the rats exhibited memory impairment while testing for their behavioral parameters via MWM and novel object recognition NOR tests. This is consistent with previous studies where ICV-STZ-treated rats showed impairment in memory without any significant changes in escape latency time in MWM[47,48] and NOR tests. Other studies showed that ICV-STZ rats had poor discrimination index and reflected no reaction to novel objects.[38,49] We subsequently studied the effects of an anticholinesterase inhibitor (donepezil), which in previous studies showed that donepezil inhibits memory deficits induced by ICV-STZ in rats.[50,51] Indeed, we also found that donepezil prevented ICV-STZ-induced memory impairment in all behavioral paradigms. Noteworthy, differences between groups in behavioral paradigms were not associated with any changes in vision and loco-motor activity, as was demonstrated by no sign between groups in swim velocity and visible platform trials. In the case of ICV-STZ injected rats, we note that STZ injection interferes with various mechanisms essential to cognitive function, such as, an increase in ROS, neuroinflammation, disruption of the mitochondrial membrane potential and function which leads to H_2O_2 production, decrease in ATP generation.[52–55] Interestingly, an increase in ROS during the metabolic processes leads to UPE increase due to electron energy level changes in a chemical reaction of electron excited species to electron ground metabolites.[18] This is accentuated particularly during hypermetabolism.[56] Moreover, when brain slices are examined under an inhibitor of the mitochondrial electron transport chain, photon emission intensity increases, indicating electron leakage from the respiratory chain.[57] Thus, these studies suggest that UPE can used to non-invasively detect a pathophysiological state (e.g., oxidative damage of living tissue) driven by the excessive production of ROS and oxidative stress.[58] In agreement with this evidence, we detected a significant elevation in UPE from the hippocampus of ICV-STZ-injected rats. We further substantiated results by finding a significant increase in MDA concentration in the hippocampus of ICV-STZ-injected rats. MDA is the index of lipid peroxidation and is known as an oxidative stress marker. The literature hypotheses that excited species are formed through a radical reaction with intracellular substances. Particularly regarding unsaturated fatty acids, excited species are generated as the result of a lipid peroxidation process.[58] The combination of previous studies and our results, in particular Pearson correlation analysis of UPE vs. MDA, leads us to conclude that elevated UPE of the hippocampus in ICV- STZ-injected rats is linked with ROS production and MDA concentration and thus UPE could be used for early detection of AD. Indeed, sporadic AD has a long latent period before the actual manifestation of disease symptoms and in MCI subjects (during this latent period) subjects exhibit significant

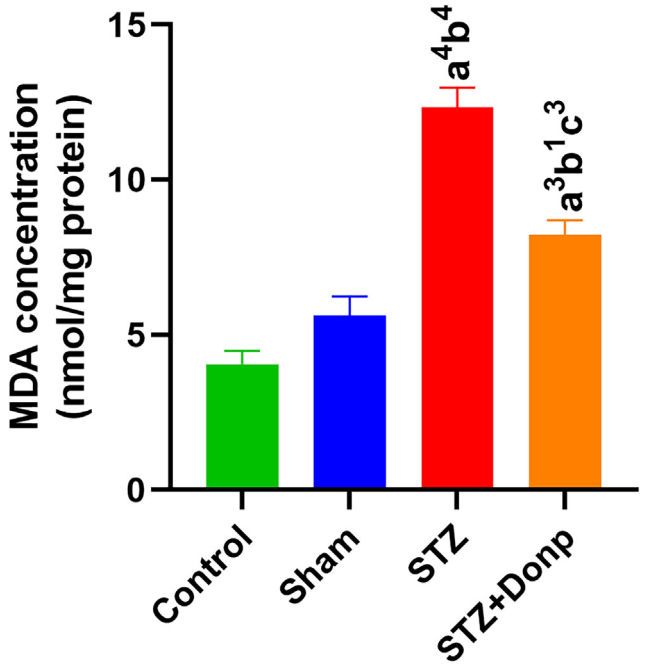

Figure 4. Representation of MDA concentration

Data were expressed as mean ± SEM (n = 8) and analyzed by one-way ANOVA followed by Tukey's multiple comparison test. (a), Compared to the control group; (b), Compared to the sham group; (c), Compared to the STZ group; 1p < 0.05, 3p < 0.001, 4p < 0.0001. STZ, Streptozotocin; Donp, Donepezil.

oxidative imbalance compared with age-matched controls. Moreover, oxidative stress occurs before forming plaques and NFTs.[59–61] In the case of ICV-STZ injected rats treated with donepezil we observed a significant reduction in UPE. This suggests that donepezil causes a decrease in ROS production and oxidative stress, as was shown by the MDA concentration decrease in donepezil-treated rats compared with the STZ group. In agreement with our results, previous studies showed that treatment with donepezil had an antioxidative effect in the ICV-STZ rat model, and the treatment decreased MDA and increased GSH levels, showing the reduction of oxidative stress in the brain of ICV-STZ rats.[39,62] ICV-STZ injection in rats causes reduced energy metabolism and synthesis of acetyl CoA, ultimately resulting in cholinergic deficiency; and, thereby, memory deficit. This process is supported by reducing ChAT activity[63] and increasing acetylcholinesterase (AChE) function[62] in the hippocampus of ICV-STZ-injected rats. Corroborating with these observations, we show an AChE activity increase in ICV-STZ-injected rats. Thus, UPE may also be correlated with metabolic systems involved in neurotransmission, as evidenced by the 61% coefficient of determination (r2) between UPE and AChE activity. A study identified associations between UPE intensity and neurotransmitter metabolites.[28]

AD is a complex condition with multiple potential causative mechanisms, including oxidative stress, chronic inflammation, impairment in insulin metabolism, and cholinergic deficits.[64] Studies have indicated an increase in acetylcholinesterase (AChE) activity along with a simultaneous decrease in ChAT activity within the hippocampal region following ICV-STZ induction. This elevated AChE activity leads to a significant reduction in cholinergic neurotransmission,[65] similar to observations in AD patients, where cholinergic transmission is disrupted. Furthermore, alterations in glucose metabolism have been reported in both sporadic AD patients and the icv-STZ model, resulting in decreased synthesis of adenosine triphosphate (ATP) and acetyl coenzyme A (acetyl-CoA). These changes contribute to cholinergic dysfunction characterized by the inhibition of ChAT activity and an increase in AChE and butyryl-cholinesterase (BChE) activities in the nervous system. The icv-STZ injection also impairs insulin signaling, leading to reduced ChAT activity and increased oxidative stress, which is associated with the upregulation of AChE in the rat brain.[39,66–69] Oxidative stress has been shown to modify biomolecules and influence AChE regulation and activity. Both AChE and BChE belong to the hydrolase family and are capable of hydrolyzing ACh at a rapid rate. In a healthy brain, BChE is responsible for approximately 20% of ACh hydrolysis. However, in AD, brain BChE activity increases, and elevated BChE levels are associated with the development of cortical and neocortical neuritic plaques. The induction of neuroinflammation through icv-STZ administration may contribute to the elevation of cholinesterase activity.[70–72] Additionally, icv-STZ administration has been shown to decrease Na+,K + -ATPase activity and increase Ca2+-ATPase activity, suggesting that disturbances in the electrolytic concentrations of Na+ and Ca2+ could lead to excitotoxicity. The increase in AChE activity may be related to faster cholinergic firing rates due to neuronal damage in the vicinity of cholinergic synapses.[73]

Donepezil, a second-generation cholinesterase inhibitor, is used therapeutically for mild to moderate dementia of AD. It inhibits AChE reversibly and non-competitively.[74] Thus, donepezil treatment can decrease the hippocampus's AChE activity in the STZ-injected rats, and this AChE metabolism reduction may be a reason for significant UPE reduction in donepezil-treated rats.

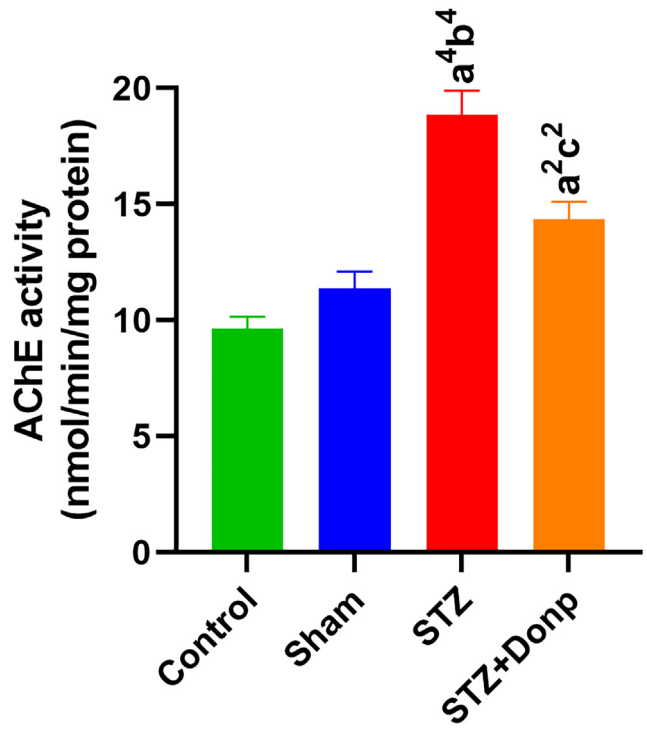

Figure 5. Representation of the AChE activity of the hippocampus

Data were expressed as mean ± SEM (n = 8) and analyzed by one-way ANOVA followed by Tukey's multiple comparison test. (a), Compared to the control group; (b), Compared to the sham group; (c), Compared to the STZ group; 1p < 0.05, 2p < 0.01, 3p < 0.001, 4p < 0.0001. STZ, Streptozotocin; Donp, Donepezil.

But activity was not reached in the sham or control group because AChE activity was evaluated six days after the last dose. Overall our results show the viability of using UPE as indicator of AD progression, however far more research will be required to classify photon emission (possibly based on photon interference patterns) and associate to specific neurophysiological processes. Nevertheless, our work contributes to a growing literature that put forward the use of UPE as a novel potential cost-effective and minimally invasive tool for monitoring spatio-temporal photon emission in diverse biological processes.[75–79] For instance, beyond our present work, UPE has been used to detect cancer, track proliferation of human esophageal carcinoma cells, monitor tumor progression[80–82] and can be used to study of normal and pathological states in various mammalian organs.[83] The advantage of UPE over traditional methods can be understood via the following example: ROS production has been analyzed by photometry, luminometry, flow cytometry, and precipitation reaction techniques.[84] All of these traditional techniques measure at only a single time point or require chemical labels. Moreover, these techniques are biopsy-dependent and not necessarily feasible for diagnostic purposes. In contrast, UPE overcomes these invasive and labor-intensive procedures and thus there is a need to develop novel UPE-based technologies for monitoring health and diseases,[85–87] such as AD as we subsequently discuss.

Discussion of envisaged BCIPC for AD

Our compelling results calls for the development of an advanced BCI photonic chip (BCIPC) for detecting, diagnosing and classifying neurodegenerative diseases (and associated syndromes), such as in AD. The envisaged BCIPC would be minimally invasive, cheap, high-speed, scalable providing high spatiotemporal resolution of brain's activity when compared to electrical chips, which have stronger limitations on the number of electrodes. The BCIPC would longitudinally capture brain's UPE and appropriate data processing would complement existing neuropathological parameters to provide an enhanced clinical assessment of AD. The envisaged BCIPC is rendered in Figure 7, and shows the possibility of connecting the BCIPC to a smart wristwatch or smartphone via its wireless connection. This technological proposal is timely, since photonic technologies are rapidly advancing. They are poised to overtake many electrical technologies due to their unique advantages, such as miniaturization, high speed, low thermal effects, and large integration capacity that allow for high yield, volume manufacturing, and lower cost. Here we provide some predictions and discuss the feasibility of the technology and its limitations for ADRDs. To implant a photonic chip for monitoring photon emissions from the hippocampus, a minimally invasive approach is preferred. This can be achieved through low-invasive chip transplantation surgery that involves placing the chip on the surface of the temporal skull. The temporal lobe, particularly the medial region, is closely related to memory and time episode formation, and is often affected earlier in dementia patients compared to other brain regions. Therefore, detecting UPE from the temporal lobe using a minimally invasive surface skull transplantation of a photonic chip is likely to be more feasible than monitoring hippocampal formation, which requires more invasive procedures and is more challenging to

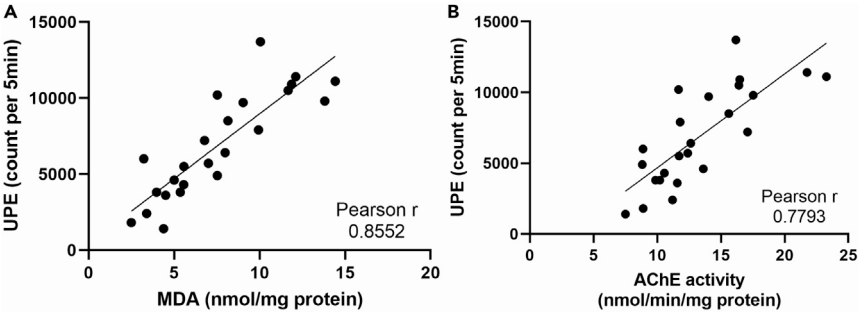

Figure 6. Correlation matrix of right hippocampus UPE vs. left hippocampus MDA concentration and Ache activity
(A) UPE vs. MDA; (B) UPE vs. AChE activity.

transplant. Using a photonic interferometer to distinguish wavelengths of UPEs, the efficiency decreases significantly. This low number of photons is still interpretable since the chip will be fitted with single-photon detectors that receive a relatively high number of photons compared to the quantum limit (i.e., 10–10^3 photons/sec). Moreover, the signal will be further discriminated from noise (e.g., dark noise and shot noise) via appropriate machine-learning training data (for a detailed discussion we refer the reader to our previously published work[3]). The integration time of the detector is estimated to be on the order of nanoseconds. Generally, biological systems exhibit UPE spectra from the near-ultraviolet and extend to the range 700–1000 nm, an optimal range for our photonic detector. Similar results may be achieved in the ultraviolet and visible spectra. These combined advantages enable for the future development of a "brain photonics" detection device to passively image the brain's spontaneous (Figure 7).

The effect of ambient light and scar on photon detection via chip

Sunlight or ambient light emits approximately 100 lumens per watt, translating to roughly. 3×10^{-2} W/cm^2. However, this value diminishes as it reaches the photonic chip. The photonic chip's front side, equipped with a photonic sensor, faces the brain's surface, while the opposite side shields against incoming ambient light. Several potential biocompatible materials can provide this shielding, such as biopolymer nanocomposites with added nanomaterials, synthetic bio-based materials derived from biomolecules and petrochemicals, aqua-Fe (III) complexes stabilized within a layered silicate scaffold, or biodegradable active layers composed of organics, perovskites, or inorganic luminescence materials. It is essential to note that ambient light in the UV and Visible range faces challenges when trying to pass through the skull. The skin acts as a barrier to UV radiation. Similarly, visible light needs to go through hair, skin, and the cranial bone, where it mostly gets absorbed by these layers. Sunlight consists of a range of wavelengths, spanning from approximately 300 nm–2500 nm. The majority of its energy is concentrated within the visible spectrum, which falls between 400 nm and 700 nm. The journey of sunlight to the brain involves passing through hair, skin, and the skull. The skin functions as a protective barrier against UV light (100–400 nm), making it improbable for UV light to directly penetrate the skull and reach the brain. Similarly, visible light (400–700 nm) struggles to penetrate all layers of hair, skin, and skull effectively to reach the brain. In contrast, near-infrared light (700–1000 nm) exhibits better penetration capabilities through the skull and head skin compared to other wavelengths. Beyond 950 nm, near-infrared light can delve deeply, even penetrating bone, the cerebrospinal fluid, and the brain. However, this falls outside the visible range of sunlight. The depth of penetration varies due to factors like tissue type and blood flow. As a result, only a small amount of sunlight manages to reach the photonic chip in the visible spectrum. To address this, a suitable material can be applied to the back of the implanted photonic chip, effectively reducing this limited penetration. Additionally, it's important to mention that despite the near-infrared (near-IR) spectrum of sunlight that can go deeper into the brain, the photonic chip cannot detect this kind of light based on the range of detection. Regarding the sensor's placement on the chip, it should be positioned very close to the brain's surface. Its primary role is to detect UPE rather than the general ambient light or the light that is around it. In order to have a minimal scar effect and efficient measurement of UPE of the hippocampus, the concept of implanting a photonic chip in close proximity to the cochlea presents an intriguing and potentially groundbreaking avenue for the measurement of UPE originating from the hippocampus. This innovative approach capitalizes on the existing anatomy of the inner ear, offering a minimally invasive pathway to access neural activity-related light emissions. By strategically positioning the photonic chip within the ear's cochlear region, it becomes possible to capture UPE associated with hippocampal function. This novel technique not only sidesteps the complexities and invasiveness of traditional cranial implantation methods but also taps into the neural-ear interface to obtain valuable insights into hippocampal activity. Importantly, given the enclosed nature of the cochlea, concerns about ambient light interference are alleviated, allowing for focused measurement of biophotonic signals. To minimize the impact of ambient light exposure, the chip's design and measurement methods can be adapted. Strategies include integrating shielding materials onto the chip, calibrating the chip to eliminate noise, controlling the measurement duration, and rigorously validating measurement accuracy and reliability.

Although surgical scars could influence oxidative stress and UPE, these effects are more noticeable in the short term. It is crucial to emphasize that the chip is designed for extended use over months and years. To ensure precise data collection and analysis, recording procedures or monitoring can begin once the potential scars have fully healed. The case of implanting a photonic chip in close proximity to the cochlea, as a neural-ear interface, is less invasive compared to direct cranial surgery. In this case, the effect of scars can be even trivial in the short term.

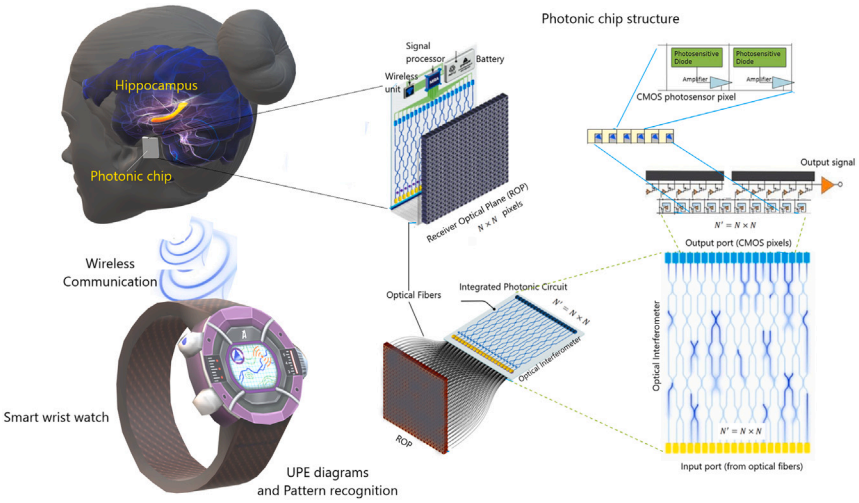

Figure 7. Potential application of a photonic chip implant for monitoring Alzheimer's disease

A schematic representation for futuristic monitoring hippocampus UPE variations and pattern recognition that may help better diagnosis of Alzheimer's disease in the short- and long-term. The photonic chip can be connected to a smart wristwatch and monitor the brain state continuously. The figure is an update from the previously published work.[3] For more details about the chip structure, see Ref.[3]

Photonic chip advantage

The photonic chip offers a significant advantage in the early detection of AD by enabling the detection of UPE signals originating from the hippocampus. This advantage stems from the fact that oxidative stress, a precursor to AD, occurs at an earlier stage, and the UPE signals possess the capability to robustly detect this early sign. There are several approaches (e.g., MRI, PET, and fluorescence imaging[88–90]) applied for AD detection and diagnosis with noninvasiveness and *in vivo* imaging capability. However, the above imaging methods are reliant on relatively costly, intricate, and stationary devices, often necessitating the injection of contrast agents during certain detection processes. In contrast, the UPE-detecting device offers mobility and eliminates the need for injections. In the advanced form of MRI, functional magnetic resonance imaging (fMRI), subjects must remain still while specific brain functions such as hearing, thinking, watching, and emotions are monitored. This monitoring is based on changes in blood supply and heat patterns. On the other hand, the UPE monitoring technique based on a chip enables the detection of a broader spectral range compared to fMRI, ranging from UV to NIR, and can be employed on freely moving subjects. At least, the long-term continuous monitoring of the brain can provide a better diagnosis method compared to the traditional methods in the short term.

Conclusion

Treatment with donepezil improved spatial and recognition memory deficits via oxidative stress regulation and AChE inhibition in ICV-STZ-injected rats. Correlations with UPE led us to the conclusion that hippocampus UPE is associated with the redox state of the tissue. Since oxidative stress is one of the primary patho-neurophysiological signatures in the progression of AD, then it stands to reason that UPE detection of the brain will provide complementary clinical parameters for AD screening and diagnosis. Moreover, UPE could be used to monitor recovery from neurodegenerative diseases upon suitable future therapeutic treatments, as suggested by our experiment involving donepezil which decreases the patho-neurophysiological signatures and in a correlated way with UPE. In the cytosol of cholinergic presynaptic neurons, Ach neurotransmitter is produced from choline and acetyl-coenzyme A (acetyl-CoA) by means of ChAT. Acetyl-CoA is a key energy precursor intermediate in all cells of our body. Acetyl-CoA is almost entirely synthesized in the brain by the pyruvate dehydrogenase multi-enzyme complex (PDHC), which supplies 97% of the energy.[91] Current AD therapy is mainly based on inhibitors of AChE by AChE inhibitors such as donepezil, rivastigmine, memantine, and galantamine, which enhance cholinergic transmission.[92] The use of donepezil is particularly promising, as it also has potent anti-inflammatory effects, inhibits neuronal death and cognitive decline, and reduces pro-inflammatory gene expression.[92] In the AD model, ICV-STZ injection induces AD disease-like symptoms that look like biomolecular, pathological, and behavioral features of AD.[93,94] ICV-STZ produces mitochondrial dysfunctions such as anomalous morphology, decreased ATP synthesis, and increased ROS generation.[94,95] This may explain why ICV-STZ injection significantly increased UPE and MDA concentrations in the hippocampus compared to the sham and control groups. Furthermore, donepezil inhibits AChE, which catalyzes the breakdown of acetylcholine (and some other choline esters that function as neurotransmitters). This may reduce mitochondrial acetyl-CoA production, i.e., mitochondria produce less acetyl-CoA, which changes the mitochondrial redox state and various mitochondrial mechanisms. As a result, these processes reduce UPE. However, the mitochondrion is the major redox, cellular signaling, and energetic hub of cells and neurons.[96] In our experiments, treatment with donepezil improved spatial and recognition memory deficits via oxidative stress regulation and AChE inhibition in ICV-STZ-injected rats. Therefore, based on the obtained results, it could be concluded that hippocampus UPE is associated with the redox state of the tissue.

Pearson correlation analysis revealed that 73% of the UPE variance could be explained by MDA concentration, while 60% of the UPE variance could be explained by AChE activity of the hippocampus. In addition, studies have suggested that mitochondria can have key roles in neurogenesis.[97–99] Increasing evidence suggests that the dysfunction of cellular organelles, particularly mitochondria, has important roles in neurodegenerative disorders.[99] These above-mentioned results and facts support the hypothesis that perturbed redox (oxidative stress) and mitochondrial mechanisms may play key roles in the development of AD. Thus, the UPE detection of the brain may be useful for a better understanding of the development of AD, its diagnosis, and the development of possible drugs. Therefore, it is possible that a photonic chip that can efficiently detect biophotons from the hippocampus could be a tool for the diagnosis or monitoring of AD. Biophoton emissions from the brain have been suggested as a potential diagnostic marker for various neurological disorders, and here we have shown that it can include AD, in which detecting changes in biophoton emissions from the hippocampus could help monitor the progression of AD. Since the results for UPE measurement are obtained with PMT in our experiments, we suggest that the photonic chip with a similar quantum efficiency as PMT can be a helpful tool for the diagnosis of AD. The CMOS quantum efficiency is about 75%, which is about three times higher than PMTs with a quantum efficiency of about 20–25%. According to the estimations in Ref. [3], the amount of total photon loss from the receiver optical plane (ROP) to the output of the optical interferometer (OI) is about 50%. The QE of CMOS at the output of the OI is estimated to be 25% in body temperature under the implant conditions to have a final SNR of about 2. However, still, further research is needed to validate the use of UPE as a diagnostic tool and determine the specific changes in UPE associated with AD, while we have now a piece of evidence to be hopeful for designing new and cheaper methods for AD diagnosis. The association between oxidative stress[100] and AD is firmly established.[101–103] Moreover, evidence suggests a connection between UPE and oxidative stress.[104,105] The mechanisms underlying the generation of ROS have also been extensively investigated.[100,106,107] Consequently, the development of a mathematical model holds promise as a framework for prospective investigations. Another avenue warranting exploration for future research is the utilization of magnetic fields. Notably, there is empirical support for the influence of magnetic field exposure on AD.[108–110] Magnetic phenomena are pervasive in biological systems, prompting the proposition of a quantum model grounded in spin correlation of radical pairs to explain these effects.[111] Furthermore, recent work by Zhang et al. demonstrated that shielding the geomagnetic field (hypomagnetic conditions) led to cognitive impairments in mice, with such impairments being correlated with ROS levels.[112] A contemporary study put forth a radical pair model to elucidate this observation.[113] Consequently, a compelling avenue emerges for investigating the impact of magnetic fields on AD, alongside the interplay between these effects, levels of ROS, and UPE within the context of AD.

STAR★METHODS

Detailed methods are provided in the online version of this paper and include the following:

- KEY RESOURCES TABLE
- RESOURCE AVAILABILITY
  - Lead contact
  - Materials availability
  - Data and code availability
- EXPERIMENTAL MODEL AND SUBJECT DETAILS
  - Animals and ethical statement
- METHOD DETAILS
  - Sample size
  - Experimental design
  - Artificial cerebrospinal fluid (aCSF) preparation
  - Intracerebroventricular cannulation
  - Morris water maze
  - Novel object recognition test
  - Hippocampus sampling
  - Detection of UPE
  - Sample preparation for biochemical analysis
  - MDA assessment
  - Acetylcholinesterase activity assessment
- QUANTIFICATION AND STATISTICAL ANALYSIS

SUPPLEMENTAL INFORMATION

Supplemental information can be found online at https://doi.org/10.1016/j.isci.2023.108744.

ACKNOWLEDGMENTS

The authors are thankful for the fruitful discussions with Prof. Christoph Simon. This article represents the outcome of international collaboration with a team of scientists, including Niloofar Sefati, a PhD candidate in Anatomical Science at Shiraz University, whose doctoral thesis has contributed to this work. S.R. acknowledges support from Ikerbasque (The Basque Foundation for Science), the Basque Government through

the BERC 2022–2025 program, and the Ministry of Science and Innovation: BCAM Severo Ochoa accreditation CEX2021-001142-S/MICIN/AEI/10.13039/501100011033 and through project RTI2018-093860-B-C21 funded by (AEI/FEDER, UE) and acronym "MathNEURO".

The work of N.S., T.E., A.Z., F.D., and M.K.G. was supported by a grant (No. 22112) from Shiraz University of Medical Sciences, Shiraz, Iran. V.S. and D.O. thank the support from the Natural Sciences and Engineering Research Council of Canada (NSERC) of Canada, the National Research Council (NRC) of Canada, and the New Frontiers in Research Fund (NFRF) a program by the Social Sciences and Humanities Research Council (SSHRC), Canada. S.R. is funded via the Basque Government through the BERC 2022–2025 program and the BCAM Severo Ochoa accreditation CEX2021-001142-S/MICIN/AEI/10.13039/501100011033 and through project RTI2018-093860- B-C21 funded by (AEI/FEDER, UE).

AUTHOR CONTRIBUTIONS

Conceptualization: T.E., A.Z., F.D., and V.S.; Data curation: N.S., T.E., and M.K.G.; Formal analysis: T.E., V.S., and M.K.G.; Funding acquisition: T.E. and V.S.; Methodology: T.E., N.S., A.Z., F.D., and M.K.G.; Project administration: T.E. and V.S.; Resources: T.E. and A.Z.; Supervision: T.E., V.S., and D.O.; Discussion: N.S., T.E., V.S., S.R., H.Z.H., and M.K.G.; Hypothesis: N.S., T.E., and V.S.; Writing an original draft: N.S., T.E., V.S., and M.K.G.; Writing a review and editing: T.E., V.S., N.C., I.B., S.R., H.Z.H., and D.O.

DECLARATION OF INTERESTS

The authors declare no competing interests.

Received: April 11, 2023
Revised: November 6, 2023
Accepted: December 7, 2023
Published: December 14, 2023

REFERENCES

1. Salari, V., Valian, H., Bassereh, H., Bókkon, I., and Barkhordari, A. (2015). Ultraweak photon emission in the brain. J. Integr. Neurosci. *14*, 419–429.
2. Esmaeilpour, T., Lotfealian, A., Anvari, M., Namavar, M., Karbalaei, N., Shahedi, A., Bókkon, I., Salari, V., and Oblak, D. (2023). Effect of methamphetamine on ultraweak photon emission and level of reactive oxygen species in male rat brain. Neurosci. Lett. *801*, 137136.
3. Salari, V., Rodrigues, S., Saglamyurek, E., Simon, C., and Oblak, D. (2021). Are Brain-Computer Interfaces Feasible with Integrated Photonic Chips? Front. Neurosci. *15*, 780344.
4. Salari, V., Bókkon, I., Ghobadi, R., Scholkmann, F., and Tuszynski, J.A. (2016). Relationship between intelligence and spectral characteristics of brain biophoton emission: correlation does not automatically imply causation. Proc. Natl. Acad. Sci. USA *113*, E5540–E5541.
5. Salari, V., Scholkmann, F., Vimal, R.L.P., Császár, N., Aslani, M., and Bókkon, I. (2017). Phosphenes, retinal discrete dark noise, negative afterimages and retinogeniculate projections: a new explanatory framework based on endogenous ocular luminescence. Prog. Retin. Eye Res. *60*, 101–119.
6. Esmaeilpour, T., Fereydouni, E., Dehghani, F., Bókkon, I., Panjehshahin, M.R., Császár-Nagy, N., Ranjbar, M., and Salari, V. (2020). An experimental investigation of ultraweak photon emission from adult murine neural stem cells. Sci. Rep. *10*, 463.
7. P. Anderson, R. Morris, D. Amaral, T. Bliss, and J. O'Keefe, eds. (2007). The Hippocampus Book (Oxford University Press).
8. Liu, N., Wang, Z., and Dai, J. (2022). Intracellular simulated biophoton stimulation and transsy- naptic signal transmission. Appl. Phys. Lett. *121*, 203701.
9. Huang, L.-K., Chao, S.-P., and Hu, C.-J. (2020). Clinical trials of new drugs for Alzheimer disease. J. Biomed. Sci. *27*, 18.
10. Bettens, K., Sleegers, K., and Van Broeckhoven, C. (2013). Genetic insights in Alzheimer's disease. Lancet Neurol. *12*, 92–104.
11. Barnes, D.E., and Yaffe, K. (2011). The projected effect of risk factor reduction on Alzheimer's disease prevalence. Lancet Neurol. *10*, 819–828.
12. Arnold, S.E., Arvanitakis, Z., Macauley-Rambach, S.L., Koenig, A.M., Wang, H.Y., Ahima, R.S., Craft, S., Gandy, S., Buettner, C., Stoeckel, L.E., et al. (2018). Brain insulin resistance in type 2 diabetes and Alzheimer disease: concepts and conundrums. Nat. Rev. Neurol. *14*, 168–181.
13. Evans, D.A., Funkenstein, H.H., Albert, M.S., Scherr, P.A., Cook, N.R., Chown, M.J., Hebert, L.E., Hennekens, C.H., and Taylor, J.O. (1989). Prevalence of Alzheimer's disease in a community population of older persons: higher than previously reported. JAMA *262*, 2551–2556.
14. Brufani, M., Filocamo, L., Lappa, S., and Maggi, A. (1997). New acetylcholinesterase inhibitors. Drugs Future *22*, 397–410.
15. Li, Q., He, S., Chen, Y., Feng, F., Qu, W., and Sun, H. (2018). Donepezil-based multi-functional cholinesterase inhibitors for treatment of Alzheimer's disease. Eur. J. Med. Chem. *158*, 463–477.
16. Mattson, M.P., Gary, D.S., and Chan, S.L. (2001). Perturbed endoplasmic reticulum function, synaptic apoptosis and the pathogenesis of Alzheimer's disease. Biochem. Soc. Symp. *67*, 151–162.
17. Wang, W., Zhao, F., Ma, X., Perry, G., and Zhu, X. (2020). Mitochondria dysfunction in the pathogenesis of Alzheimer's disease: recent advances. Mol. Neurodegener. *15*, 30.
18. Pospíšil, P., Prasad, A., and Rác, M. (2014). Role of reactive oxygen species in ultra-weak photon emission in biological systems. J. Photochem. Photobiol., B *139*, 11–23.
19. Tafur, J., Van Wijk, E.P.A., Van Wijk, R., and Mills, P.J. (2010). Biophoton detection and low-intensity light therapy: a potential clinical partnership. Photomed. Laser Surg. *28*, 23–30.
20. Havaux, M., Triantaphylidès, C., and Genty, B. (2006). Autoluminescence imaging: a non-invasive tool for mapping oxidative stress. Trends Plant Sci. *11*, 480–484.
21. Prasad, A., and Pospíšil, P. (2013). Towards the two-dimensional imaging of spontaneous ultra-weak photon emission from microbial, plant and animal cells. Sci. Rep. *3*, 1–8.
22. Tsuchida, K., Iwasa, T., and Kobayashi, M. (2019). Imaging of ultraweak photon emission for evaluating the oxidative stress of human skin. J. Photochem. Photobiol., B *198*, 111562.
23. Esmaeilpour, T., Fereydouni, E., Dehghani, F., Bókkon, I., Panjehshahin, M.R., Császár-Nagy, N., Ranjbar, M., and Salari, V. (2020). An experimental investigation of ultraweak photon emission from adult murine neural stem cells. Sci. Rep. *10*, 463.
24. Scordino, A., Baran, I., Gulino, M., Ganea, C., Grasso, R., Niggli, J.H., and Musumeci, F. (2014). Ultra-weak delayed luminescence in cancer research: A review of the results by the ARETUSA equipment. J. Photochem. Photobiol., B *139*, 76–84.
25. Sun, Y., Wang, C., and Dai, J. (2010). Biophotons as neural communication signals demonstrated by in situ biophoton autography. Photochem. Photobiol. Sci. *9*, 315–322.

26. Rizzo, N.R., Hank, N.C., and Zhang, J. (2016). Detecting presence of cardiovascular disease through mito- chondria respiration as depicted through biophotonic emission. Redox Biol. *8*, 11–17.
27. Mittal, M., Siddiqui, M.R., Tran, K., Reddy, S.P., and Malik, A.B. (2014). Reactive oxygen species in inflammation and tissue injury. Antioxid. Redox Signal. *20*, 1126–1167.
28. He, M., van Wijk, E., van Wietmarschen, H., Wang, M., Sun, M., Koval, S., van Wijk, R., Hankemeier, T., and van der Greef, J. (2017). Spontaneous ultra-weak photon emission in correlation to inflammatory metabolism and oxidative stress in a mouse model of collagen-induced arthritis. J. Photochem. Photobiol., B *168*, 98–106.
29. Yang, M., Ding, W., Liu, Y., Fan, H., Bajpai, R.P., Fu, J., Pang, J., Zhao, X., and Han, J. (2017). Ultra-weak photon emission in healthy subjects and patients with type 2 diabetes: evidence for a non-invasive diagnostic tool. Photochem. Photobiol. Sci. *16*, 736–743.
30. Zhao, X., Pang, J., Fu, J., Wang, Y., Yang, M., Liu, Y., Fan, H., Zhang, L., and Han, J. (2017). Spontaneous photon emission: A promising non-invasive diagnostic tool for breast cancer. J. Photochem. Photobiol., B *166*, 232–238.
31. Winblad, B., Amouyel, P., Andrieu, S., Ballard, C., Brayne, C., Brodaty, H., Cedazo-Minguez, A., Dubois, B., Edvardsson, D., Feldman, H., et al. (2016). Defeating Alzheimer's disease and other dementias: a priority for European science and society. Lancet Neurol. *15*, 455–532.
32. Kodamullil, A.T., Zekri, F., Sood, M., Hengerer, B., Canard, L., McHale, D., and Hofmann-Apitius, M. (2017). Trial watch: Tracing investment in drug development for Alzheimer disease. Nat. Rev. Drug Discov. *16*, 819.
33. Kitazawa, M., Medeiros, R., and Laferla, F.M. (2012). Transgenic mouse models of Alzheimer disease: developing a better model as a tool for therapeutic interventions. Curr. Pharm. Des. *18*, 1131–1147.
34. Salkovic-Petrisic, M. (2008). Amyloid cascade hypothesis: is it true for sporadic Alzheimer's disease. Period. Biol. *110*, 17–25.
35. Kamat, P.K., Kalani, A., Rai, S., Tota, S.K., Kumar, A., and Ahmad, A.S. (2016). Streptozotocin intracerebroventricular-induced neurotoxicity and brain insulin resistance: a therapeutic intervention for treatment of sporadic Alzheimer's disease (sAD)-like pathology. Mol. Neurobiol. *53*, 4548–4562.
36. Plaschke, K., and Hoyer, S. (1993). Action of the diabetogenic drug streptozotocin on glycolytic and glycogenolytic metabolism in adult rat brain cortex and hippocampus. Int. J. Dev. Neurosci. *11*, 477–483.
37. Lannert, H., and Hoyer, S. (1998). Intracerebroventricular administration of streptozotocin causes long- term diminutions in learning and memory abilities and in cerebral energy metabolism in adult rats. Behav. Neurosci. *112*, 1199–1208.
38. Shoham, S., Bejar, C., Kovalev, E., Schorer-Apelbaum, D., and Weinstock, M. (2007). Ladostigil prevents gliosis, oxidative–nitrative stress and memory deficits induced by intracerebroventricular injection of streptozotocin in rats. Neuropharmacology *52*, 836–843.
39. Sharma, B., Singh, N., and Singh, M. (2008). Modulation of celecoxib-and streptozotocin-induced exper- imental dementia of Alzheimer's disease by pitavastatin and donepezil. J. Psychopharmacol. *22*, 162–171.
40. Lannert, H., and Hoyer, S. (1998). Intracerebroventricular administration of streptozotocin causes long-term diminutions in learning and memory abilities and in cerebral energy metabolism in adult rats. Behav. Neurosci. *112*, 1199–1208.
41. Kamat, P.K., Kalani, A., Rai, S., Tota, S.K., Kumar, A., and Ahmad, A.S. (2016). Streptozotocin intracerebroventricular-induced neurotoxicity and brain insulin resistance: A therapeutic intervention for treatment of sporadic Alzheimer's disease (sAD)-like pathology. Mol. Neurobiol. *53*, 4548–4562.
42. Grieb, P. (2016). Intracerebroventricular streptozotocin injections as a model of Alzheimer's disease: in search of a relevant mechanism. Mol. Neurobiol. *53*, 1741–1752.
43. Henneman, W.J.P., Sluimer, J.D., Barnes, J., van der Flier, W.M., Sluimer, I.C., Fox, N.C., Scheltens, P., Vrenken, H., and Barkhof, F. (2009). Hippocampal atrophy rates in Alzheimer disease: added value over whole brain volume measures. Neurology *72*, 999–1007.
44. Barnes, D.E., and Yaffe, K. (2011). The projected effect of risk factor reduction on Alzheimer's disease prevalence. Lancet Neurol. *10*, 819–828.
45. Moreira, P.I., Duarte, A.I., Santos, M.S., Rego, A.C., and Oliveira, C.R. (2009). An integrative view of the role of oxidative stress, mitochondria and insulin in Alzheimer's disease. J. Alzheimers Dis. *16*, 741–761.
46. Cho, H.J., Kim, S.K., Jin, S.M., Hwang, E.M., Kim, Y.S., Huh, K., and Mook-Jung, I. (2007). IFN-γ-induced BACE1 expression is mediated by activation of JAK2 and ERK1/2 signaling pathways and direct binding of STAT1 to BACE1 promoter in astrocytes. Glia *55*, 253–262.
47. Awasthi, H., Tota, S., Hanif, K., Nath, C., and Shukla, R. (2010). Protective effect of curcumin against intracere- bral streptozotocin induced impairment in memory and cerebral blood flow. Life Sci. *86*, 87–94.
48. Saxena, G., Bharti, S., Kamat, P.K., Sharma, S., and Nath, C. (2010). Melatonin alleviates memory deficits and neuronal degeneration induced by intracerebroventricular administration of streptozotocin in rats. Pharmacol. Biochem. Behav. *94*, 397–403.
49. Liu, P., Zou, L.B., Wang, L.H., Jiao, Q., Chi, T.Y., Ji, X.F., and Jin, G. (2014). Xanthoceraside attenuates tau hyper-phosphorylation and cognitive deficits in intracerebroventricular-streptozotocin injected rats. Psychopharmacology *231*, 345–356.
50. Saxena, G., Patro, I.K., and Nath, C. (2011). ICV STZ induced impairment in memory and neuronal mi- tochondrial function: a protective role of nicotinic receptor. Behav. Brain Res. *224*, 50–57.
51. Agrawal, R., Tyagi, E., Shukla, R., and Nath, C. (2011). Insulin receptor signaling in rat hippocampus: a study in STZ (ICV) induced memory deficit model. Eur. Neuropsychopharmacol *21*, 261–273.
52. Ishrat, T., Khan, M.B., Hoda, M.N., Yousuf, S., Ahmad, M., Ansari, M.A., Ahmad, A.S., and Islam, F. (2006). Coenzyme Q10 modulates cognitive impairment against intracerebroventricular injection of streptozotocin in rats. Behav. Brain Res. *171*, 9–16.
53. Hoyer, S. (2000). Brain glucose and energy metabolism abnormalities in sporadic Alzheimer disease. Causes and consequences: an update. Exp. Gerontol. *35*, 1363–1372.
54. Rai, S., Kamat, P.K., Nath, C., and Shukla, R. (2013). A study on neuroinflammation and NMDA recep- tor function in STZ (ICV) induced memory impaired rats. J. Neuroimmunol. *254*, 1–9.
55. Javed, H., Khan, M.M., Ahmad, A., Vaibhav, K., Ahmad, M.E., Khan, A., Ashafaq, M., Islam, F., Siddiqui, M.S., Safhi, M.M., and Islam, F. (2012). Rutin prevents cogni- tive impairments by ameliorating oxidative stress and neuroinflammation in rat model of sporadic dementia of Alzheimer type. Neuroscience *210*, 340–352.
56. Adamo, A.M., Llesuy, S.F., Pasquini, J.M., and Boveris, A. (1989). Brain chemiluminescence and oxidative stress in hyperthyroid rats. Biochem. J. *263*, 273–277.
57. Kobayashi, M., Takeda, M., Sato, T., Yamazaki, Y., Kaneko, K., Ito, K., Kato, H., and Inaba, H. (1999). In vivo imaging of spontaneous ultraweak photon emission from a rat's brain correlated with cerebral energy metabolism and oxidative stress. Neurosci. Res. *34*, 103–113.
58. Cadenas, E., Boveries, A., and Chance, B. (1984). Low-level chemiluminescence of biological systems. In Free Radicals in Biology, W.A. Pryor, ed. (Academic Press), pp. 211–242.
59. Mufson, E.J., Chen, E.Y., Cochran, E.J., Beckett, L.A., Bennett, D.A., and Kordower, J.H. (1999). Entorhinal cortex β- amyloid load in individuals with mild cognitive impairment. Exp. Neurol. *158*, 469–490.
60. Markesbery, W.R., Schmitt, F.A., Kryscio, R.J., Davis, D.G., Smith, C.D., and Wekstein, D.R. (2006). Neuropathologic substrate of mild cognitive impairment. Arch. Neurol. *63*, 38–46.
61. Price, J.L., McKeel, D.W., Jr., Buckles, V.D., Roe, C.M., Xiong, C., Grundman, M., Hansen, L.A., Petersen, R.C., Parisi, J.E., Dickson, D.W., et al. (2009). Neuropathology of nondemented aging: presumptive evidence for preclinical Alzheimer disease. Neurobiol. Aging *30*, 1026–1036.
62. Agrawal, R., Tyagi, E., Shukla, R., and Nath, C. (2009). A study of brain insulin receptors, AChE activ- ity and oxidative stress in rat model of ICV STZ induced dementia. Neuropharmacology *56*, 779–787.
63. Blokland, A., and Jolles, J. (1993). Spatial learning deficit and reduced hippocampal ChAT activity in rats after an ICV injection of streptozotocin. Pharmacol. Biochem. Behav. *44*, 491–494.
64. de la Monte, S.M. (2012). Contributions of brain insulin resistance and deficiency in amyloid-related neurodegeneration in Alzheimer's disease. Drugs *72*, 49–66.
65. Agrawal, M., Perumal, Y., Bansal, S., Arora, S., and Chopra, K. (2020). Phycocyanin alleviates ICV-STZ induced cognitive and molecular deficits via PI3-Kinase dependent pathway. Food Chem. Toxicol. *145*, 111684.
66. Frölich, L., Blum-Degen, D., Bernstein, H.G., Engelsberger, S., Humrich, J., Laufer, S., Muschner, D., Thalheimer, A., Türk, A.,

Hoyer, S., et al. (1998). Brain insulin and insulin receptors in aging and sporadic Alzheimer's disease. J. Neural. Transm. *105*, 423–438.
67. Shoham, S., Bejar, C., Kovalev, E., Schorer-Apelbaum, D., and Weinstock, M. (2007). Ladostigil prevents gliosis, oxidative-nitrative stress and memory deficit induced by intracerebroventricular injection of streptozotocin in rats. Neuropharmacology *52*, 836–843.
68. Lester-Coll, N., Rivera, E.J., Soscia, S.J., Doiron, K., Wands, J.R., and de la Monte, S.M. (2006). Intracerebral streptozotocin model of type 3 diabetes: relevance to sporadic Alzheimer's disease. J. Alzheimers Dis. *9*, 13–33.
69. Biasibetti, R., Tramontina, A.C., Costa, A.P., Dutra, M.F., Quincozes-Santos, A., Nardin, P., Bernardi, C.L., Wartchow, K.M., Lunardi, P.S., and Gonçalves, C.A. (2013). Green tea (-) epigallocatechin-3-gallate reverses oxidative stress and reduces acetylcholinesterase activity in a streptozotocin-induced model of dementia. Behav. Brain Res. *236*, 186–193.
70. Mesulam, M.M., and Geula, C. (1994). Butyrylcholinesterase reactivity differentiates the amyloid plaques of aging from those of dementia. Ann. Neurol. *36*, 722–727.
71. Bazelyansky, M., Robey, E., and Kirsch, J.F. (1986). Fractional diffusion - limited component of reactions catalyzed by acetylcholinesterase. Biochemistry *25*, 125–130.
72. Guillozet, A.L., Smiley, J.F., Mash, D.C., and Mesulam, M.M. (1997). Butyrylcholinesterase in the life cycle of amyloid plaques. Ann. Neurol. *42*, 909–918.
73. Gutierres, J.M., Carvalho, F.B., Schetinger, M.R.C., Marisco, P., Agostinho, P., Rodrigues, M., Rubin, M.A., Schmatz, R., da Silva, C.R., de P Cognato, G., et al. (2014). Anthocyanins restore behavioral and biochemical changes caused by streptozotocin-induced sporadic dementia of Alzheimer's type. Life Sci. *96*, 7–17.
74. scarpini, E., Schelterns, P., and Feldman, H. (2003). Treatment of Alzheimer's disease; current status and new perspec- tives. Lancet Neurol. *2*, 539–547.
75. Van Wijk, R., Van Wijk, E.P.A., Wiegant, F.A.C., and Ives, J. (2008). Free radicals and low-level photon emission in human pathogenesis: state of the art. Indian J. Exp. Biol. *46*, 273–309.
76. Rastogi, A., and Pospísil, P. (2011). Spontaneous ultraweak photon emission imaging of oxidative metabolic processes in human skin: effect of molecular oxygen and antioxidant defense system. J. Biomed. Opt. *16*, 096005.
77. Burgos, R.C.R., Schoeman, J.C., Winden, L.J.V., Červinková, K., Ramautar, R., Van Wijk, E.P.A., Cifra, M., Berger, R., Hankemeier, T., and Greef, J.v.d. (2017). Ultra-weak photon emission as a dynamic tool for monitoring oxidative stress metabolism. Sci. Rep. *7*, 1229.
78. Yang, M., Van Wijk, E., Pang, J., Yan, Y., van der Greef, J., Van Wijk, R., and Han, J. (2019). A bridge of light: Toward chinese and western medicine perspectives through ultraweak photon emissions. Glob. Adv. Health Med. *8*, 2164956119855930.
79. He, M., Sun, M., van Wijk, E., van Wietmarschen, H., van Wijk, R., Wang, Z., Wang, M., Hankemeier, T., and van der Greef, J. (2016). A Chinese literature overview on ultra-weak photon emission as promising technology for studying system-based diagnostics. Complement. Ther. Med. *25*, 20–26.
80. Amano, T., Kobayashi, M., Devaraj, B., Usa, M., and Inaba, H. (1995). Ultraweak biophoton emission imaging of transplanted bladder cancer. Urol. Res. *23*, 315–318.
81. Takeda, M., Tanno, Y., Kobayashi, M., Usa, M., Ohuchi, N., Satomi, S., and Inaba, H. (1998). A novel method of assessing carcinoma cell proliferation by biophoton emission. Cancer Lett. *127*, 155–160.
82. Takeda, M., Kobayashi, M., Takayama, M., Suzuki, S., Ishida, T., Ohnuki, K., Moriya, T., and Ohuchi, N. (2004). Biophoton detection as a novel technique for cancer imaging. Cancer Sci. *95*, 656–661.
83. Boveris, A., Cadenas, E., Reiter, R., Filipkowski, M., Nakase, Y., and Chance, B. (1980). Organ chemiluminescence: noninvasive assay for oxidative radical reactions. Proc. Natl. Acad. Sci. USA *77*, 347–351.
84. Bylund, J., Björnsdottir, H., Sundqvist, M., Karlsson, A., and Dahlgren, C. (2014). Measurement of respiratory burst products, released or retained, during activation of professional phagocytes. Methods Mol. Biol. *1124*, 321–338.
85. Prasad, A., and Pospíšil, P. (2011). Linoleic acid-induced ultra-weak photon emission from Chlamydomonas reinhardtii as a tool for monitoring of lipid peroxidation in the cell membranes. PLoS One *6*, e22345.
86. Rastogi, A., and Pospíšil, P. (2013). Ultra-weak photon emission as a non-invasive tool for the measure- ment of oxidative stress induced by UVA radiation in Arabidopsis thaliana. J. Photochem. Photobiol., B *123*, 59–64.
87. Ives, J.A., van Wijk, E.P.A., Bat, N., Crawford, C., Walter, A., Jonas, W.B., van Wijk, R., and van der Greef, J. (2014). Ultraweak photon emission as a non-invasive health assessment: a systematic review. PLoS One *9*, e87401.
88. Xie, X., Bian, J., Song, Y., Liu, G., Zhao, Y., Zhang, J., Li, Y., Jiao, X., Wang, X., and Tang, B. (2023). In situ fluorescence imaging reveals contribution of cerebral hydroxyl radicals in hyperhomocysteinemia-induced Alzheimer-like dementia. Anal. Chem. *95*, 9872–9880.
89. Xie, X., Liu, Y., Liu, G., Zhao, Y., Liu, J., Li, Y., Zhang, J., Jiao, X., Wang, X., and Tang, B. (2022). Two-photon fluorescence imaging of the cerebral peroxynitrite stress in Alzheimer's disease. Chem. Commun. *58*, 6300–6303.
90. Xie, X., Liu, G., Niu, Y., Xu, C., Li, Y., Zhang, J., Jiao, X., Wang, X., and Tang, B. (2021). Dual-channel imaging of amyloid- plaques and peroxynitrite to illuminate their correlations in alzheimer's disease using a unimolecular two-photon fluorescent probe. Anal. Chem. *93*, 15088–15095.
91. Szutowicz, A., Bielarczyk, H., Jankowska-Kulawy, A., Pawełczyk, T., and Ronowska, A. (2013). Acetyl-CoA the key factor for survival or death of cholinergic neurons in course of neurodegenerative diseases. Neurochem. Res. *38*, 1523–1542.
92. Xu, P.Y., Li, S.M., and Mo, M.S. (2015). Progress in mechanisms of acetylcholinesterase inhibitors and memantine for treatment of Alzheimer's disease. Neuroimmunol. Neuroinflamm. *2*, 274–280.
93. Grieb, P. (2016). Intracerebroventricular streptozotocin injections as a model of Alzheimer's disease: in search of a relevant mechanism. Mol. Neurobiol. *53*, 1741–1752.
94. Park, J., Won, J., Seo, J., Yeo, H.G., Kim, K., Kim, Y.G., Jeon, C.Y., Kam, M.K., Kim, Y.H., Huh, J.W., et al. (2020). Streptozotocin Induces Alzheimer's disease-Like pathology in hippocampal neuronal cells via CDK5/Drp1-mediated mitochondrial fragmentation. Front. Cell. Neurosci. *14*, 235.
95. Guo, X.D., Sun, G.L., Zhou, T.T., Wang, Y.Y., Xu, X., Shi, X.F., Zhu, Z.Y., Rukachaisirikul, V., Hu, L.H., and Shen, X. (2017). LX2343 alleviates cognitive impairments in AD model rats by inhibiting oxidative stress-induced neuronal apoptosis and tauopathy. Acta Pharmacol. Sin. *38*, 1104–1119.
96. Aon, M.A., and Camara, A.K.S. (2015). Mitochondria: hubs of cellular signaling, energetics and redox balance. A rich, vibrant, and diverse landscape of mitochondrial research. Front. Physiol. *6*, 94.
97. Unger, M.S., Marschallinger, J., Kaindl, J., Höfling, C., Rossner, S., Heneka, M.T., Van der Linden, A., and Aigner, L. (2016). Early changes in hippocampal neurogenesis in transgenic mouse models for Alzheimer's disease. Mol. Neurobiol. *53*, 5796–5806.
98. Brunetti, D., Dykstra, W., Le, S., Zink, A., and Prigione, A. (2021). Mitochondria in neurogenesis: Implications for mitochondrial diseases. Stem Cell. *39*, 1289–1297.
99. Zhang, S., Zhao, J., Quan, Z., Li, H., and Qing, H. (2022). Mitochondria and other organelles in neural development and their potential as therapeutic targets in neurodegenerative diseases. Front. Neurosci. *16*, 853911.
100. Sies, H., Belousov, V.V., Chandel, N.S., Davies, M.J., Jones, D.P., Mann, G.E., Murphy, M.P., Yamamoto, M., and Winterbourn, C. (2022). Defining roles of specific reactive oxygen species (ROS) in cell biology and physiology. Nat. Rev. Mol. Cell Biol. *23*, 499–515.
101. Huang, W.J., Zhang, X., and Chen, W.W. (2016). Role of oxidative stress in Alzheimer's disease. Biomed. Rep. *4*, 519–522.
102. Tönnies, E., and Trushina, E. (2017). Oxidative Stress, Synaptic Dysfunction, and Alzheimer's Disease. J. Alzheimers Dis. *57*, 1105–1121.
103. Butterfield, D.A., and Halliwell, B. (2019). Oxidative stress, dysfunctional glucose metabolism and Alzheimer disease. Nat. Rev. Neurosci. *20*, 148–160.
104. Tsuchida, K., Iwasa, T., and Kobayashi, M. (2019). Imaging of ultraweak photon emission for evaluating the oxidative stress of human skin. J. Photochem. Photobiol., B *198*, 111562.
105. Tsuchida, K., and Kobayashi, M. (2020). Oxidative stress in human facial skin observed by ultraweak photon emission imaging and its correlation with biophysical properties of skin. Sci. Rep. *10*, 9626.
106. Demidchik, V. (2015). Mechanisms of oxidative stress in plants: From classical chemistry to cell biology. Environ. Exp. Bot. *109*, 212–228.
107. Dickinson, B.C., and Chang, C.J. (2011). Chemistry and biology of reactive oxygen species in signaling or stress responses. Nat. Chem. Biol. *7*, 504–511.

108. Liu, X., Zuo, H., Wang, D., Peng, R., Song, T., Wang, S., Xu, X., Gao, Y., Li, Y., Wang, S., et al. (2015). Improvement of spatial memory disorder and hippocampal damage by exposure to electromagnetic fields in an Alzheimer's disease rat model. PLoS One *10*, e0126963.
109. Davanipour, Z., and Sobel, E. (2009). Long-term exposure to magnetic fields and the risks of Alzheimer's disease and breast cancer: Further biological research. Pathophysiology *16*, 149–156.
110. García, A.M., Sisternas, A., and Hoyos, S.P. (2008). Occupational exposure to extremely low frequency electric and magnetic fields and Alzheimer disease: a meta-analysis. Int. J. Epidemiol. *37*, 329–340.
111. Zadeh-Haghighi, H., and Simon, C. (2022). Magnetic field effects in biology from the perspective of the radical pair mechanism. J. R. Soc. Interface *19*, 20220325.
112. Zhang, B., Wang, L., Zhan, A., Wang, M., Tian, L., Guo, W., and Pan, Y. (2021). Long-term exposure to a hypomagnetic field attenuates adult hippocampal neurogenesis and cognition. Nat. Commun. *12*, 1174.
113. Rishabh, R., Zadeh-Haghighi, H., Salahub, D., and Simon, C. (2022). Radical pairs may explain reactive oxygen species-mediated effects of hypomagnetic field on neurogenesis. PLoS Comput. Biol. *18*, e1010198.
114. Halliwell, B., and Chirico, S. (1993). Lipid peroxidation: its mechanism, measurement, and significance. Am. J. Clin. Nutr. *57*, 715S–724S. discussion 724S-725S.
115. Tsikas, D. (2017). Assessment of lipid peroxidation by measuring malondialdehyde (MDA) and relatives in biological samples:Analytical and biological challenges. Anal. Biochem. *524*, 13–30.
116. Draper, H.H., and Hadley, M. (1990). Malondialdehyde determination as index of lipid peroxidation. Methods Enzymol. *186*, 421–431.
117. Ellman, G.L., Courtney, K.D., Andres, V., Jr., and Featherstone, R.M. (1961). A new and rapid colorimetric determination of acetylcholinesterase activity. Biochem. Pharmacol. *7*, 88–95.
118. Bradford, M.M. (1976). A rapid and sensitive method for the quantitation of microgram quantities of protein utilizing the principle of protein-dye binding. Anal. Biochem. *72*, 248–254.

STAR★METHODS

KEY RESOURCES TABLE

REAGENT or RESOURCE	SOURCE	IDENTIFIER
Chemicals, peptides, and recombinant proteins		
NaCl	Sigma-Aldrich	Cat# S5886
KCl	Sigma-Aldrich	Cat# P5405
MgCl	Sigma-Aldrich	Cat# M8266
CaCl	Sigma-Aldrich	Cat# C4901
Dextrose	Sigma-Aldrich	Cat# D9434
Stereptozocin	Sigma-Aldrich	Cat# S0130
Acetylthiocholine iodide	Sigma-Aldrich	Cat# A5751
Dithiobisnitrobenzoic acid	Sigma-Aldrich	Cat# D8130
Phosphate buffered saline	Sigma-Aldrich	Cat# P4417
2-Thiobarbituric acid	Sigma-Aldrich	Cat# T5500
Trichloroacetic acid	Sigma-Aldrich	Cat# T4885
1,1,3,3-Tetraethoxypropane	Sigma-Aldrich	Cat# T9889
Donepezil hydrochloride	Sigma-Aldrich	Cat# D6821
Experimental models: Organisms/strains		
Rat: Sprague-Dawley; 7–9 week old males	Comparative and Experimental Medical Center of the Shiraz University of Medical Sciences	Biomed1@sums.ac.ir
Biological samples		
Adult rat hippocampus tissue	Collected in the lab	N/A
Critical commercial assays		
Pierce Bradford Protein Assay Kit	Thermo Fisher	Cat# 23200
Software and algorithms		
EthoVision XT 14	Noldus	https://www.noldus.com/ethovision-xt
GEN 5 3.05	Agilent	https://www.agilent.com.cn/en/support/biotek-software-releases
Prism 8.0	GraphPad	https://www.graphpad.com/
G*power 3.1.9.7	Heinrich-Heine-Universität Düsseldorf	https://www.psychologie.hhu.de/arbeitsgruppen/allgemeine-psychologie-und-arbeitspsychologie/gpower
Other		
Orion Lab Star PH111 Bench pH Meters	Thermo Fisher Scientific	Cat# LSTAR1118
Mechanical Pipette	Eppendorf Research plus	Cat# 3123000098
Microplate reader	Agilent	BioTek Synergy H1
T 10 basic ULTRA-TURRAX	IKA	Cat# 0003737000
Microliter syringe	Hamilton	Cat# 80300
Dual Lab Standard Stereotaxic Instrument, Rat	Stoelting	Cat# 51603
Photomultiplier tube	Hamamatsu	Cat# R6095
G.G.104 converter	Parto Tajhiz Besat	https://rghp.ir

RESOURCE AVAILABILITY

Lead contact

Further information and requests for resources should be directed to and will be fulfilled by the lead contact Niloofar Sefati (Niloofar.Sefati89@gmail.com).

Materials availability

This study did not generate new materials.

Data and code availability

Raw data and any additional information about this paper is available from the lead contact upon request.

EXPERIMENTAL MODEL AND SUBJECT DETAILS

The whole method is graphically represented in Figure S1. The details are as follows:

Animals and ethical statement

In this study, 7–9 week old/adult Sprague-Dawley male rats (220–250 g), were obtained from the Comparative and Experimental Medical Center of the Shiraz University of Medical Sciences. All rats were housed under standard conditions (temperature: 22 ± 2 °c, relative humidity: 50%, with a 12-h light/dark cycle) and had free access to laboratory food and water. The animals were subjected to an acclimatization period of one week before the beginning of the experiments. To prevent seasonal disturbances, experiments were started on all groups at the same time. All procedures in the study were based on the National Institutes of Health (NIH) guidelines for the care and use of laboratory animals (NIH Publications No. 8023, revised 1978) and were approved by the Ethics Committee of the Shiraz University of Medical Sciences (approval number: IR.SUMS.REC.1400.191).

METHOD DETAILS

Sample size

To determine the appropriate sample size, we conducted a power analysis using the G*Power 3.1.9.7 software, focusing on the novel object recognition (NOR) test due to its highest recorded standard deviation among the outcomes. By extrapolating the effect size (0.69) from our prior NOR findings, we performed a power analysis for a one-way ANOVA F-test. This analysis revealed that approximately 32 participants would be the minimum sample size needed to achieve a statistical power of 0.9, assuming an alpha of 0.05 and an effect size of 0.69.

Experimental design

The rats were divided with simple randomized sampling into four groups (n = 8), including Control, Sham, STZ, and STZ+Donp groups. The Control group underwent without any intervention. Sham and experimental groups underwent ICV cannulation of both lateral ventricles. To produce the ICV-STZ rat model and memory impairment in rats, after cannulation, ICV injection of STZ on days 1 and 3 of the experiment was done. For this purpose, 3 mg/kg STZ (Sigma, St. Louis, USA) was dissolved in 10 μL sterile saline 0.9% and injected slowly into both lateral ventricles (each side 5μL). The Sham rats were treated identically with 10 μL sterile saline 0.9%. One week after the second injection of STZ, the intraperitoneal (IP) treatments were initiated on the rats until day 23. Sham and STZ group received 0.2 mL saline 0.9% daily/IP, and the STZ+Donp group received 0.75 mg/kg donepezil daily/IP. From days 24–29 of the experiment, rats were subjected to MWM and NOR tests. Finally, on day 30, the rats were dislocated, and their brains were removed (see Figure S2).

Artificial cerebrospinal fluid (aCSF) preparation

Artificial cerebrospinal fluid (aCSF) was prepared as follows: (in mmol/L) 147 mM NaCl, 2.9 mM KCl, 1.6 mM MgCl2, 1.7 mM CaCl2, and 2.2 mM dextrose. Then solution PH adjusted to 7.4 with PH meter (Orion Lab Star, Thermo Fisher Scientific).

Intracerebroventricular cannulation

On the zero-day of the experiment, we carried out ICV cannulation of both lateral ventricles. Briefly, rats were anesthetized with an IP injection of ketamine HCl 10% (70 mg/kg) and xylazine HCl 2% (10 mg/kg). Their heads were placed in a stereotaxic frame (Dual Lab Standard Stereotaxic Instrument, Stoelting) and a midline incision was made sagittally in the scalp. The bregma boundary was visible after removing the remaining tissue. Holes were drilled in the skull with a dental handpiece with a burr size of 1 mm on both sides over the lateral ventricles using the following coordinates from Paxinos atlas (0.8 mm posterior to bregma, 1.5 mm lateral to the sagittal line). Two cannulas with a height of 3 mm were inserted in these holes. Then, holes and cannula were covered with dental cement to fix the position. For ICV injection, the injection needle with 3.5 mm height was connected to the 10 μL syringe (Hamilton, Bonaduz, Switzerland) by a short piece of narrow polyethylene tube. The needle was inserted into the tip of the cannula.

Morris water maze

We employed the Morris Water Maze (MWM) to assess spatial memory. MWM test was performed from days 24–27 of the experiment. The maze consisted of a circular pool (160 cm in diameter, 60 cm in height), and up to 35 cm in height, it is filled with water (the temperature at 22 ± 10C). The pool is geographically divided into four-quarters, equal north, south, east, and west, and in each quarter of the circle, a point is intended to leave the animal in the water. A transparent platform (diameter, 10 cm) was positioned in the middle of the target quadrant and submerged approximately 1 cm below the water's surface. All rats underwent four daily trials for three consecutive days for spatial learning assessment. The starting quadrant was changed each day. If the rat failed to find the hidden platform within 60 s, it was guided to the platform by the experimenter. The rats stood on the platform for 10 s for spatial examination of the platform zone. Then, they were removed from the pool into the cage and rested for 1 min under a heater inside the cage. A probe trial was performed 24 h after the last acquisition trial to assess spatial memory. In this phase, the hidden platform was removed, and rats were abandoned from the opposite quadrant of the target quadrant into the water and given 60 s to swim in the pool. A visible platform trial was performed after the probe trial to check the rat's vision and platform perception. Time to reach the platform (escape latency), time spent in the target quadrant, the number of platform site crossings, and swimming speeds were automatically estimated with a video tracking system (EthoVision XT, Noldus Information Technology) for measuring mobility accurately; the software must be calibrated.

Novel object recognition test

On the 28th day of the experiment, recognition memory was evaluated by a novel object recognition test. The testing apparatus was a box with dimensions 65 × 65 × 45 cm this test was performed for two days. On the first day, to familiarize themselves with the test box, the rats are located in the test box for 5 min without any objects. On the second day in the familiarization phase, two similar objects were placed in two corners of the box, and the rats were placed in the box for 5 min to explore objects. Then the rats returned to the cage. After 60 min, the rats were retrial in the box for the testing phase, and one of the familiar objects was replaced with a new object. The time spent to check each object was measured for 5 min. The animals were evaluated when facing, sniffing, or biting the object. some equipment, such as a test box and objects, were cleaned with 70% ethanol between trials. Eventually, the discrimination index (the spent time identifying a novel object divided by the spent total time exploring either object) was measured for recognition memory assessment.

Hippocampus sampling

Finally, the rats cervical dislocated on day 30, and the brains were rapidly removed. Then, the right and left brain hemispheres separated, the right hippocampus was dissected for biophoton emission evaluations, and the left one was stored at −80 C for MDA and AChE activity measurements (see Figure S3).

Detection of UPE

In this study, UPE were detected with the photomultiplier tube (PMT) placed in a dark box in a dark room. PMT is an intensely sensitive detector amplifying entrance photons from a field of view to electrical signals. The PMT was connected to the G.G.104 (Parto-Tajhiz-Besat co - PTB) converter, which was also connected to the laptop for data to be digitally visible. A photon counting system (R6095 Hamamatsu Photonics K.K., Electron Tube Center, Hamamatsu, Japan) was used to observe time-dependent photon emission intensity. PMT provides detection of photons in the range of 300–700 nm wavelength, with the highest quantum efficiency (30%) at 420 nm. The collecting gate time from the PMT was set at 1s. Dark noise was detected with the number of counts in an empty dark box for 5 min (c.p.5 min) before sample UPE detection and subtracted from the results. Noise is reduced by modifying the upper and lower thresholds via PMT software. The distance between the sample and the PMT sensor was 0.5 cm. In each trial period, the medium's emission and then the UPE of samples were measured in a 5 min period. The right hippocampus was dissected and transferred to a 3 cm Petri dish containing oxygenated aCSF (O2 95%, CO2 5%), which was placed under the sensor. For declining any possible delayed luminescence, Petri dish was placed in the darkroom for 10 min.[23]

Sample preparation for biochemical analysis

The left hippocampus was removed, weighed, and homogenized in the 10-fold ice-cold phosphate buffer saline. The homogenizing was accomplished using Homogenizer (IKA T10 basic, Germany) apparatus for about 3 m. Next, centrifuging (12000 rpm) at 4°C for 5 m was performed, and the supernatant was isolated for the following assessments.

MDA assessment

Oxidative stress can lead to damage in various biological molecules, with proteins and DNA being particularly susceptible to early injury, while lipid peroxidation typically occurs at a later stage in the injury process. Malondialdehyde (MDA) serves as a marker for lipid peroxidation, and its levels are indicative of the degree of oxidative stress.[114,115] To measure MDA, 200 μL of supernatant was added to 800 μL of TCA 20%/TBA 0.8% solution. Then, the microtubes were placed in an incubator at 87°C for 1 h away from the sunlight. After 1 h, color produced during the reaction of thiobarbituric acid (TBA) with MDA and the microtubes were located on ice for 2–3 min. After chilling, they were centrifuged at 4000 rpm for 10 min. Afterward, 200 μL of each microtube solution was transferred to the microplate, and absorption of supernatants was read by an Elisa plate reader (Bio-Tek Instruments, Inc) at a wavelength of 532 nm. MDA concentration was estimated using 1,1,3,3-tetra ethoxy propane as a standard.[116] Results expressed as nmol/mg protein.

Acetylcholinesterase activity assessment

The activity of AChE was carried out according to the Ellman method, which uses acetylthiocholine as a substrate. To measure the activity 0.4 mL aliquot of the supernatant was added to a cuvette containing 2.6 mL of phosphate buffer (pH 8.0, 0.1 M) Then 100 μL Dithiobisnitrobenzoic acid (DTNB) 0.01 M were added. The absorbance was measured at 412 nm; when this had stopped increasing, the photometer slit was opened so that the absorbance was set to zero then 20 μL Acetylthiocholine iodide 0.075 M was added. Changes in absorbance per min was recorded and the activity rate calculated by following formula:

$$R = \Delta A/1.36\ (104) * 1/\ (400 / 3120)\ C0$$

where R = rate, in moles substrate hydrolyzed per min per g of tissue; ΔA = change in absorbance per min; C0 = original concentration of tissue (mg/mL). Thiocholine, produced by AChE, reacts with DTNB to form a colorimetric product proportional to the AChE activity and expressed as nmol/min/mg protein.[117] Protein concentration of supernatant was measured by protein assay kit (Thermo Fisher) according to the method of Bradford.[118]

QUANTIFICATION AND STATISTICAL ANALYSIS

Data were presented as the mean ± SEM, and $p < 0.05$ was considered statistically significant (four group; n = 8). The normality of data was evaluated by the Kolmogorov-Smirnov test. To assess escape latency and swim velocity (Morris water maze) changes during the time, a two-way repeated-measures analysis of variance (TWRM-ANOVA) was done. Also, for other parameters, one-way ANOVA followed by Tukey's post hoc test was utilized for comparing various groups. In the NOR test, exploration time during the testing phase was analyzed by paired t-test. To evaluate relation of the hippocampus UPE with MDA concentration and AChE activity, a Pearson correlation analysis was done. All statistical analyses were performed using GraphPad software (Prism Software Inc., San Diego, CA, USA).